



Original Research Article

Effect of Lithium Salts on the Optical Properties of Poly Acrylonitrile/Poly Methyl Methacrylate Blends

Raad H. Khudher*^{ID}, Ahmad A. Hasan^{ID}

Department of Physics, College of Science, University of Baghdad, Baghdad, Iraq

ARTICLE INFO

Article history

Submitted: 2022-05-02

Revised: 2022-07-09

Accepted: 2021-08-13

Manuscript ID: CHEMM-2208-1587

Checked for Plagiarism: Yes

Language Editor:

Dr. Nadereh Shirvani

Editor who approved publication:

Dr. Sami Sajjadifar

DOI:10.22034/CHEMM.2022.354600.1587

KEYWORDS

PAN/PMMA blends

Optical properties of polymer blends

Optical constants

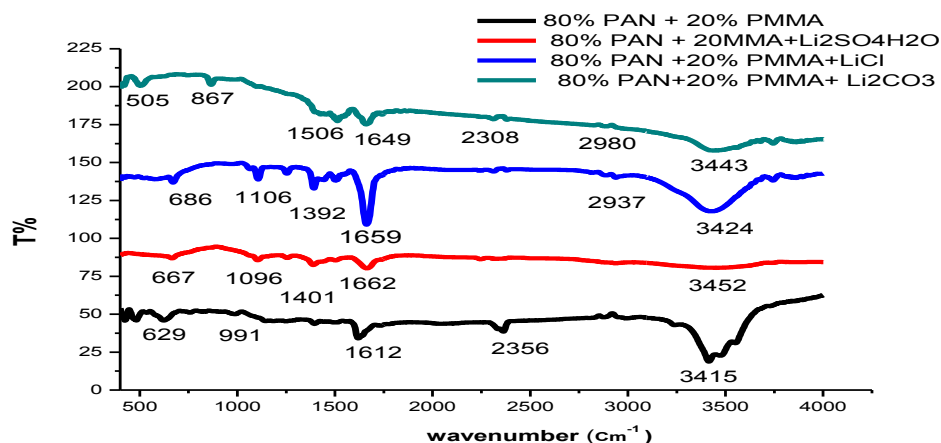
Solid electrolyte

Lithium Salts

ABSTRACT

Polymer blends from Poly Acrylonitrile/Poly Methyl Methacrylate (PAN/PMMA) with different blend ratios (80/20, 75/25, 70/30, 65/35, and 60/40) wt% undoped and doped with various lithium (Li) salts (LiCO_3 , $\text{Li}_2\text{SO}_4\cdot\text{H}_2\text{O}$, and LiCl) at 20 wt %. Different techniques were employed to investigate the composition and optical properties of the prepared blend samples undoped and doped with Lithium salts like FT-IR and UV-Visible spectroscopies. The optical properties analysis declared that the energy gap increased from (4.0 eV to 4.20 eV) by increasing of PMMA ratio from 20 to 40 wt %. In contrast, the energy gap reduced and shifted toward the low energy side by adding lithium salts; the minimum energy gap value was 2 eV obtained from 65 % PAN and 35 % PMMA doped with Li_2CO_3 . The optical constants were determined and plotted as a function of wavelength in the range (of 100-1100) nm. The general results showed that the optical constants (n , ϵ_r , and ϵ_i) for undoped blends increased with the PMMA ratio from 20 to 35 wt%. In contrast, all-optical constants were grown with the addition of lithium salts.

GRAPHICAL ABSTRACT



* Corresponding author: Raad H. Khudher

✉ E-mail: Forat. almuswyrad@gmail.com

© 2022 by SPC (Sami Publishing Company)

Introduction

In recent years polymeric materials such as PAN and PMMA have acquired a broad interest from scientific and technological researchers because of their importance in manufacturing applications [1]. Increased attention in studying polymer electrolytes continuously in applications in Lithium batteries and electronics [2]. The development of a polymer system with high ionic conductivity stability is the congenital objective in polymer research; Polymer electrolytes envisage the advantage of solid electrolytes as well as the property of liquid electrolytes [3, 4]. Hence, the polymer electrolyte owns less crystallinity as the conduction in polymer electrolytes is through the non-crystalline domain of the polymer salt system [3]. PMMA has an amorphous and a good candidate for non-linear optical application in communications technology. Using PMMA as a polymer host material in developing polymer-based electrolytes has given high ionic conductivity at sub-ambient temperature and good solvent retention ability to date [5, 6]. PAN resins are copolymers made from mixtures of monomers with acrylonitrile as the main monomer. PAN has low density, high ionic conductivity, good thermal stability, and good compatibility with lithium metal has high strength and modulus of elasticity. PAN is soluble in polar solvents, such as DMF [7]. Lithium salts for the investigation of polymer-ceramic composite electrolytes include LiNSO_2F , LiFSi , $\text{LiN}(\text{C}_2\text{F}_5\text{SO}_2)_2$, LiTFSi , LiClO_4 , LiCl , Li_2CO_3 , $\text{Li}_2\text{SO}_4 \cdot \text{H}_2\text{O}$, and LiNO_3 , etc. [8]. These lithium salts are also widely used in liquid electrolytes due to their high solvability, good electrochemical stability, high thermal stability, and ability to promote the formation of a stable solid-electrolyte interphase (SEI) [9]. Nimali et al. [10] investigated a supercapacitor electrode material derived from an immiscible polymer blend comprising polyacrylonitrile (PAN) and polymethyl methacrylate (PMMA). PAN was used as the carbonizing polymer, while PMMA was used as the sacrificial polymer. Rajendran et al. [11] have prepared composite electrolyte films consisting of poly(vinyl chloride),

poly(acrylonitrile), ethylene carbonate, LiClO_4 , and TiO_2 particles by solution casting technique. The effect of inorganic filler on the conductivity of the composite polymer electrolyte was studied. A conductivity of $7.57 \times 10^{-5} \text{ S cm}^{-1}$ is achieved at room temperature for the composition PVC-PAN- LiClO_4 -EC (4.8-19.2-8-68). In contrast, it improves two orders of magnitude ($4.46 \times 10^{-3} \text{ S cm}^{-1}$) upon dispersing fine particles of TiO_2 as inert filler. The role of the ceramic phase is to reduce the melting temperature, which is ascertained from the Thermo gravimetric /differential thermal analysis by Bernab et al. [12]. Presents the results of research on the method of obtaining PAN/PANI membranes using the phase inversion method from a solution in DMF, following two methods: 1) dissolving both polymers (PAN and PANI) and then coagulating in water or an aqueous solution of CSA and 2) forming the membranes from polyacrylonitrile solution and coagulation in water, followed by a coating of CSA with a solution of TFE. The membranes obtained as a result of the experiment were tested for physical and chemical properties, transport properties, surface morphology, degree of dispersion of composite components, and sensitivity to the presence of dilute acids and bases. FT-IR micro spectroscopy and scanning electron microscopy were used to study the surface morphology. Athal et al. [13] prepared Polyacrylonitrile PAN by electrospinning in normal conditions at room temperature. The PAN nanofibers were investigated by XRD and SEM techniques. Optical properties of the thin film of Polyacrylonitrile (PAN) nanofibers were studied by the transmission and absorption spectra at room temperature within the wavelength of (300-700 nm) optical energy gap and other parameters were calculated using Tauc relation. The dispersion relationship of the refractive index was computed. In the present work, we tend to investigate the effect of blends ratio and the addition of different lithium salts on the FT-IR spectrum and the optical properties of PAN-PMMA blend samples.

Materials and Methods

The solution casting technique prepared all blend samples. The blend samples were prepared from polyacrylonitrile (PAN) (Mackun Comp.) with an average molecular weight of 150,000 and poly methyl methacrylate (PMMA) (Aldrich Comp.) with an average molecular weight of 120,000. Lithium salts used in this work were LiCO_3 , $\text{Li}_2\text{SO}_4\text{H}_2\text{O}$, and LiCl supplied from Aldrich company.

Appropriate quantities of each polymer according to blend weight ratios percentage PAN/PMMA (80/20, 75/25, 70/30, 65/35, and 60/40) wt% were dissolved in 25 mL distilled DMF (supplied by THOMAS BAKER – CHEM Limited, India) and then stirred with magnetic stirrer continuously for six h at 70 °C to an obtained homogeneous solution then it was poured in a glass Petridis and

then left to evaporate the solvent in a temperature-controlled oven at 50 °C for 48 h to get dried blend sample.

In order to prepare blend composite samples, a constant lithium salts weight ratio of 20% from Li_2CO_3 , $\text{Li}_2\text{SO}_4\text{H}_2\text{O}$, and LiCl was dissolved in 15 mL of DMF and then added to the blend solution as in the procedure above to get PAN/PMMA blend samples doped with 20% lithium salts as shown in Figure 1. UV/Visible spectroscopy measurements were carried out using UV-1650PC SHIMADZU UV-Visible Spectrophotometer, which operates in the wavelength range of (180-1100 nm). The structural changes and the composition effect in the prepared blend samples were studied using a FUSE TYPE (220-230-240) mV FTIR-SHIMADZU spectrophotometer operating in the wave number range of 400-4000 cm^{-1} .

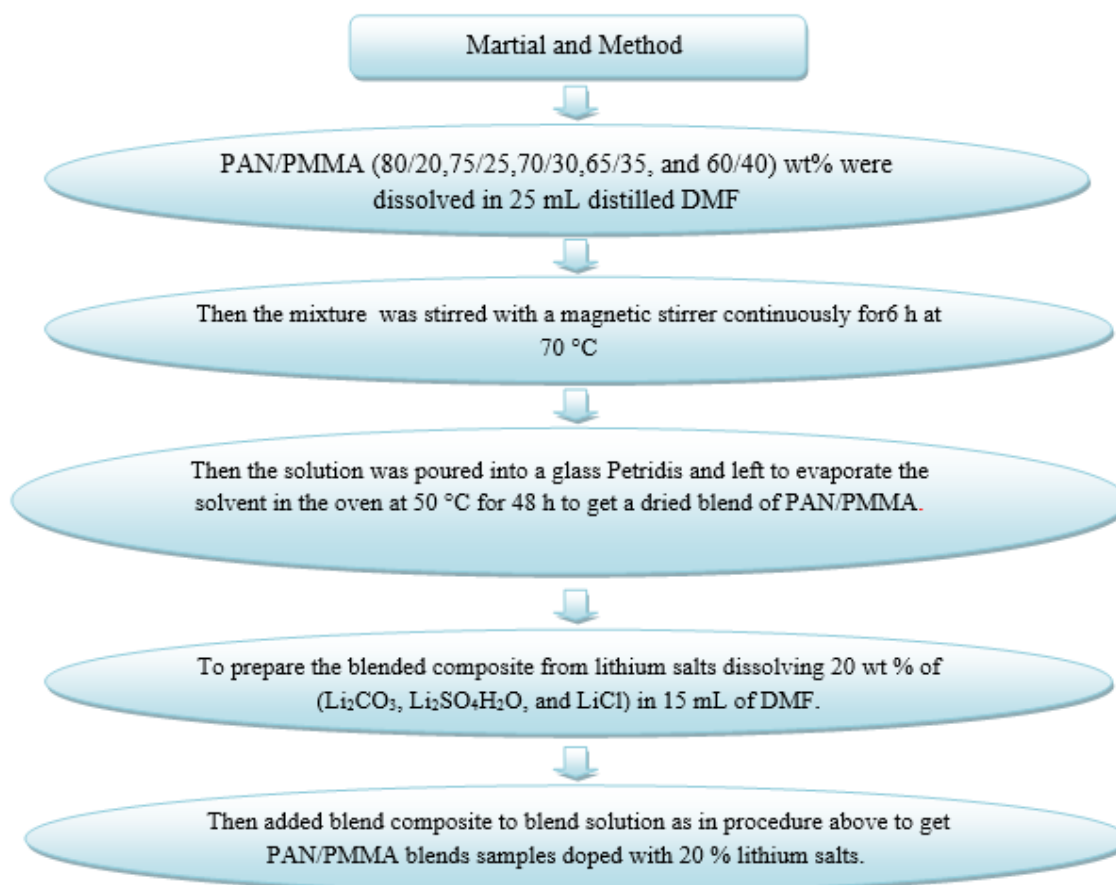


Figure 1: Schematic diagram in the experimental work for the preparation of PAN/PMMA blends with Lithium salts

The relationship between absorbed light intensity (I) by material and the intensity of incident light (I_0) is given by [14].

$$I = I_0 e^{-\alpha t} \quad (1)$$

Where (t) is the thickness of the matter and (α) is the absorption coefficient [15]

$$\alpha = 2.303 \frac{A_b}{t} \quad (2)$$

Where (A_b) is the absorption of the material and (t) is the sample thickness in cm.

The absorption coefficient (α) is defined as the material's capability to absorb light.

The optical energy gap (E_g), is related to the absorption coefficient (α) and the energy of photon by tauc equation [16]

$$(\alpha h\nu) = \beta(h\nu - E_g)^r \quad (3)$$

Where (β) is constant, (r) depends on the transition types, $r=0.5, 3/2$ for direct allowed and forbidden transition, $r= 2, 3$ for indirect allowed and forbidden transition, respectively. The refractive index (n) is the ratio between the velocity of light in a vacuum to that of material, and can be calculated using the relations:

$$R = \frac{(n-1)^2}{(n+1)^2} \quad (4)$$

$$n = \frac{(1+\sqrt{R})}{(1-\sqrt{R})} \quad (5)$$

Where (R) is the reflectance. The extinction coefficient (k), which determines the energy lose in materials as a result of interaction between the light and the medium, can be measured using the following relation [17]

$$k = \frac{\alpha \lambda}{4\pi} \quad (6)$$

where (λ) is the wavelength

The complex dielectric constant ($\epsilon^* = (\epsilon_r + i\epsilon_i)$) characterizes the optical properties of the solid material, where (ϵ_r) real part and (ϵ_i) imaginary part of the dielectric constant, and can be determined by the following equations [18].

$$\epsilon = \epsilon_r - i\epsilon_i \quad (7)$$

$$\epsilon_r = n^2 - k^2 \quad (8)$$

The calculation of these two parts provides information about the loss factor [19].

Results and Discussion

FT-IR analysis

FT-IR is an activity tool to study the local structural changes in polymers. The infrared spectra of these materials vary according to their installation and aid in confirming the complex formation between polymer matrices and the interaction among the various constituents. The FT-IR spectra of PAN-PMMA with different blend ratios undoped and doped with Li_2CO_3 , $\text{Li}_2\text{SO}_4 \cdot \text{H}_2\text{O}$ and LiCl salts are shown in Figure 2. The FT-IR spectrum exhibits some characteristic band assignments of stretching and of O-H, C-H, C=C, and C-O groups of PAN-PMMA blends with different wt% ratios, undoped and doped with many types of lithium salts. During the comparison of PMMA/PAN blend at different wt % with types of lithium salts, the spectral characteristics changes are seen, and the corresponding band positions and their assignment to the absorption can be seen also. Band O-H exhibited at 3415, 3424, 3415, 3443, 3452, 3471, 3550, 3429, 3416, and 3409 cm^{-1} was due to the intermolecular hydrogen bond stretching vibration and the presence of different concentration ratio PMMA/PAN and concentration kinds salts constant ratio, the weak absorption at most 2946, 2928, 2996, 2973, 2971, 2980, 2935, 2929, and 2873 cm^{-1} attributed to different types of lithium salts such as stretching C-H. The intensity of the sharp band at 1668, 1630, 1659, 1660, 1640, 1673, 1666, 1625, and 1611 cm^{-1} due to C=C stretching in all the complexes in Figure 2 can be observed. These changes may be due to the interaction of types of lithium salts with the blend polymer. The change in the appearance and the intensity of the lines reveal the complex formation of blend polymer (PAN+PMMA) with doped types of lithium salts, or this may be due to the association through the redistribution of charge accompanying the formation of ionic pairs and aggregation than attributed interaction of types of lithium salts with the blend polymer (PAN+PMMA). The

absorption peaks of groups at 609~686 cm^{-1} and 1086~1181 cm^{-1} belonged to C-O stretching and

C-C and C-O bending found in all samples shown in Figure 2 [20].

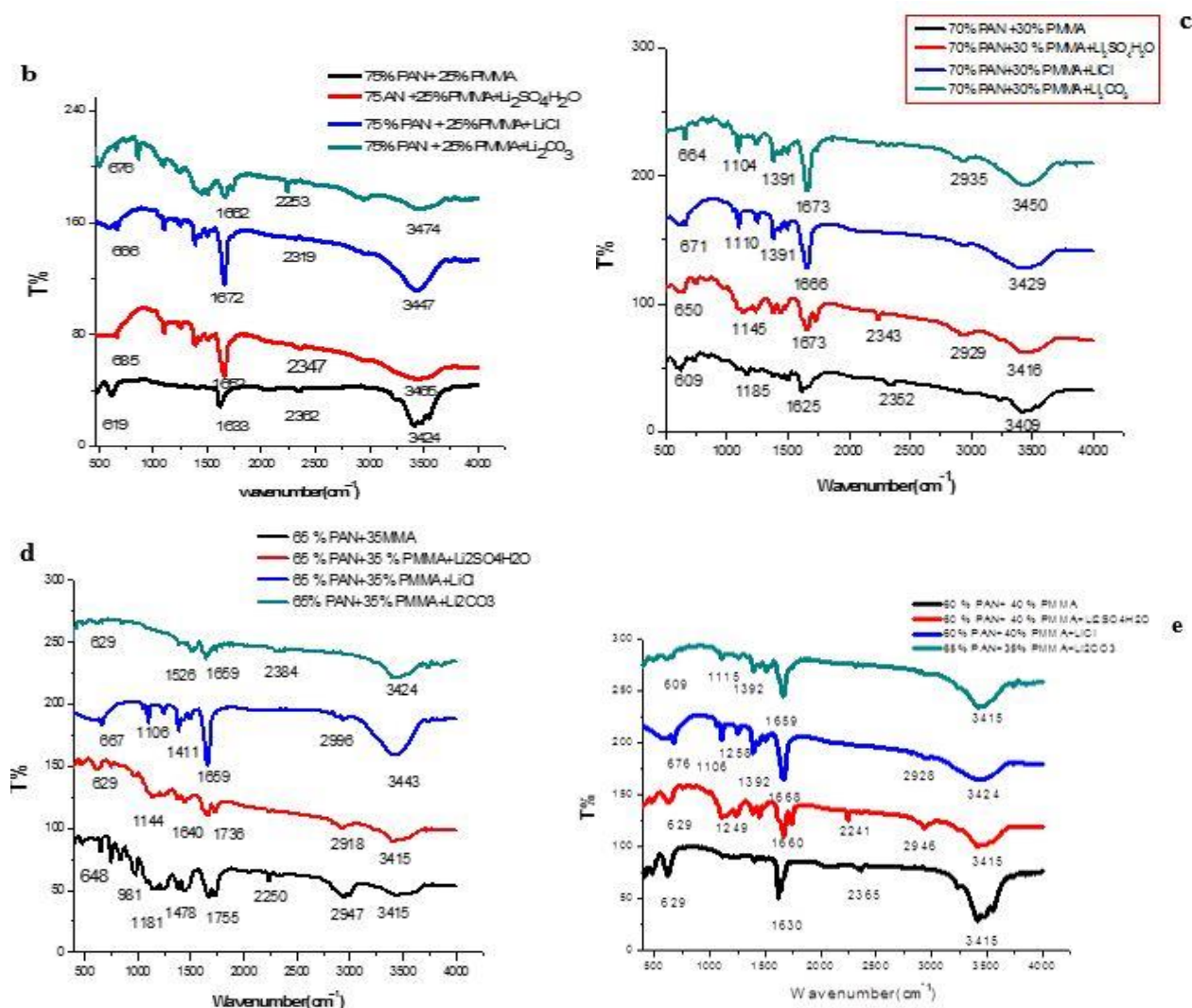


Figure 2: FT-IR of different wt.% of PAN/ PMMA blend undoped and doped with Lithium salt

Optical properties

The optical properties of different concentrations of PAN/PMMA blends, undoped and doped with different lithium salts Li_2CO_3 , $\text{Li}_2\text{SO}_4\cdot\text{H}_2\text{O}$, and LiCl including the measurements of absorbance, optical energy gap E_g and optical constants such as refractive index (n), extinction coefficient (k), and dielectric constant (ϵ).

Optical transition

The UV-Vis absorbance spectra in the region 180-1100 nm for different concentrations of PMMA/PAN blends with various lithium salts, including Li_2CO_3 , $\text{Li}_2\text{SO}_4\cdot\text{H}_2\text{O}$, and LiCl spectra for all films decreased with increasing wavelength, while the absorption increased with increasing

lithium salts Li_2CO_3 , $\text{Li}_2\text{SO}_4\cdot\text{H}_2\text{O}$, and LiCl , absorbance increases is an irregular increase in all samples, and this is due to the different concentrations of polymer blends (PAN+PMMA). Either polymer-doped mixtures with lithium salts by weight by 20%, its absorbance will be higher than the undoped polymer blend (PAN/PMMA) because the doped samples are darker than the other samples doped with salts lithium. The incident radiation at the lithium salts ions is combined with the polymer chains, which absorb the shortest wavelengths, as shown in Figure 3. It is clear from the Figure 3 that the absorption spectra for all films decreased with increasing wavelength while the absorption increased with the addition of lithium salts to the polymer blend

(PMMA/PAN). This indicated the formation of blend and the filler [21]. charge transfer complexes between the polymer

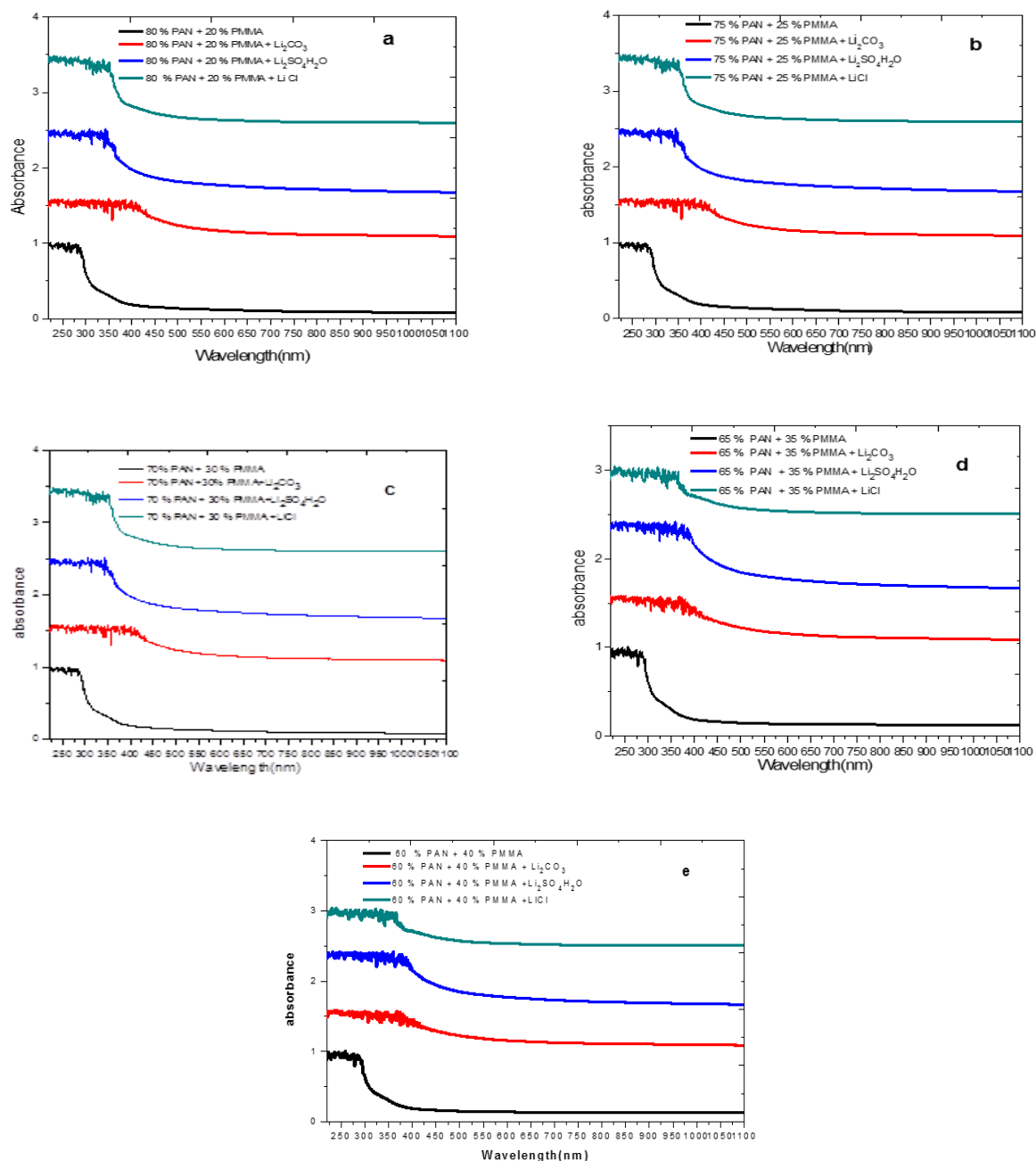


Figure 3: The absorbance as a function of wavelength for (PAN /PMMA) blends with different blends ratios undoped and doped with 20% of Li_2CO_3 , $\text{Li}_2\text{SO}_4\text{H}_2\text{O}$, and LiCl

Optical energy gap for (PAN/PMMA) blends undoped and doped with different lithium salts

Figure 4 shows the relation between $(\alpha h\nu)^{1/r}$ for different weight blend ratios for (PAN/PMMA) blends and with doping with lithium salts (Li_2CO_3 , $\text{Li}_2\text{SO}_4\text{H}_2\text{O}$, and LiCl) as a function of photon energy on drawing a straight line from the upper part of the curve toward the (x) axis. At the value

$(\alpha h\nu)^{1/r} = 0$, an energy gap was gotten for the allowed indirect transition. The obtained values are shown in Table 1. It can be seen that the values of the energy gap increase by the effect of increasing the PMMA ratio while they reduce by adding different lithium salts to the PAN-PMMA polymer blend. Indeed, the energy gap grows up from 4 eV to 4.2 eV by increasing PMMA from

20% to 40%. The increase of the energy gap values by the increase of PMMA ratio attributed to the addition of wide band gap polymer like PMMA to lower energy gap polymer like PAN, the energy gap of PMMA = 4.9 eV [21]. The effect of adding Li_2CO_3 salt among the salts to the polymer blends is more pronounced than other types of salts in all-polymer blends except $\text{Li}_2\text{SO}_4\cdot\text{H}_2\text{O}$ doped (75%PAN+ 25%PMMA). So, the addition of different lithium salts to the PAN/PMMA blend leads to a lowering energy gap. In contrast, the

energy gap of PAN is = 3.92 eV [22], while the shift of the energy gap to the low energy side is attributed to the creation of onsite levels in the energy gap. The transition, in this case, is conducted in two stages that involve the transition of an electron from the valence band to the local levels [23]. The minimum optical energy gap (2 eV) value was obtained for blend sample 75%PAN80+25%PMMA) doped lithium carbonate as shown in Table 1.

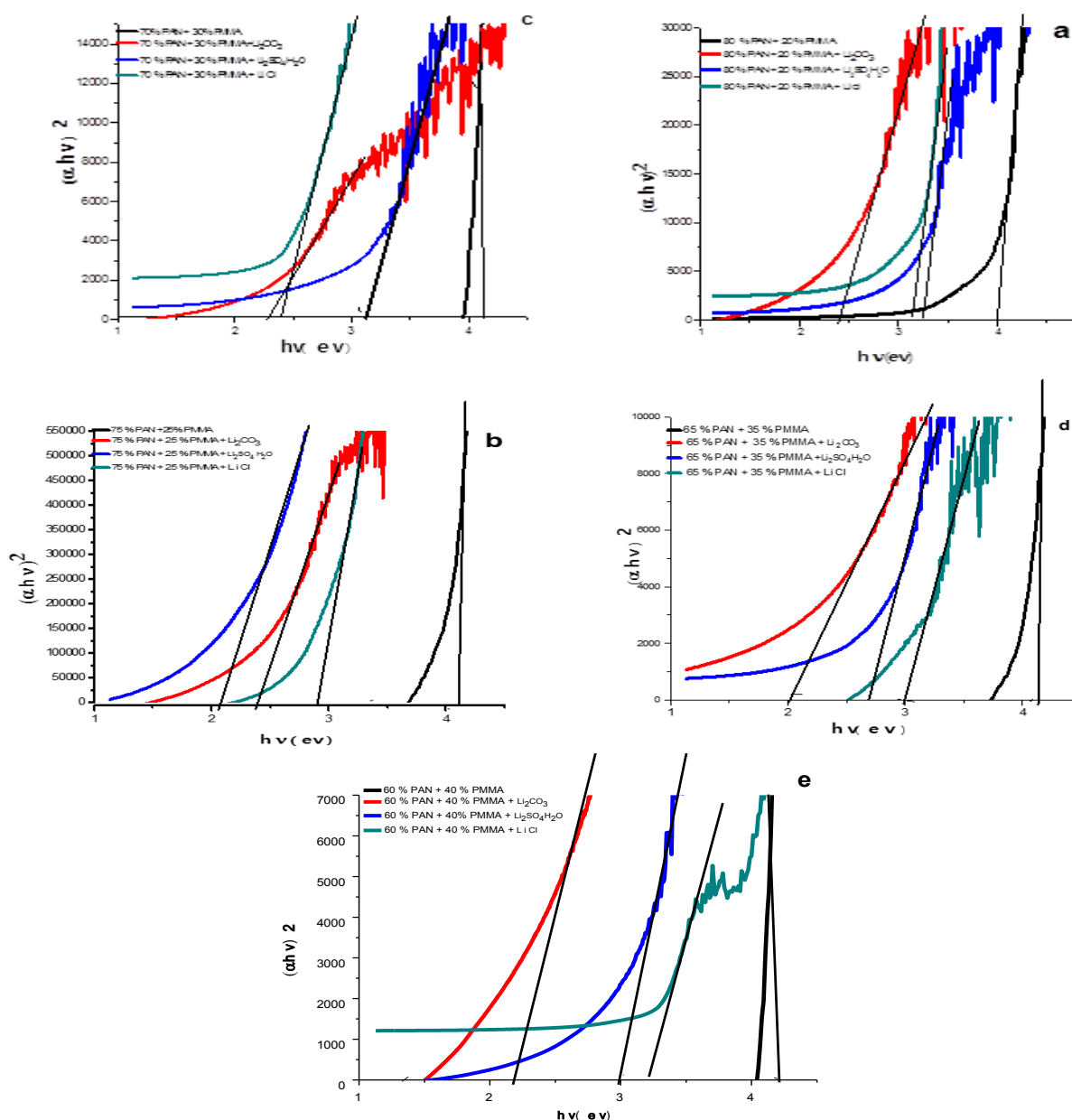


Figure 4: Variation of $(\alpha h\nu)^2$ with photon energy ($h\nu$) of (PAN+ PMMA) blends with different weight blend ratios undoped and doped with 20% of Li_2CO_3 , $\text{Li}_2\text{SO}_4\cdot\text{H}_2\text{O}$, and LiCl

Refractive index (n) of PAN/PMMA blends with different weight blends ratios undoped and doped with different Lithium salts

The wavelength (λ) dependence of the refractive index (n) of PAN+PMMA films with different blends undoped and doped with Li_2CO_3 , $\text{Li}_2\text{SO}_4\cdot\text{H}_2\text{O}$, and LiCl is shown in Figure 5. It is obvious that when the wavelength increased for all samples of polymer blend doped lithium salts, the (n) values take a straight-line likeness constant of the incident photon for all samples, while the refractive index for undoped (PAN+PMMA) at different blends ratios to decrease as the wavelength is increased. The refractive indices values for all doped lithium salts samples are higher than that of undoped ones, as shown in Figure 4 and Table 1. The variation of the refractive index (increasing and decreasing was related to the reduction and growth of the transmittance values, and this which implies an increase in the energy gap. The

decrease in the refractive index reflects the increase in transmittance, i.e., the sample become more transparent, the incident wavelength, as expected from the simultaneous increase in the energy gap.

whereas in contrast, the reduction in the refractive index reflects the transmittance increase, i.e., the sample becomes more opaque to the incident wavelength, as expected from the simultaneous decrease in the energy gap. The increase in the refractive index is related to the increase in packing density (the material becomes opaquer), which causes the velocity of light in the medium to decrease [24, 25]. The vibration in the refractive index spectra in the short wavelength range is attributed to the introduction of filler to the host polymer blend PAN-PMMA, which observed for polymer blends with low PMMA ratios, i.e., 20, 25, 30 wt.%. The vibration disappears completely at a PMMA ratio of 35 wt.% but returns to show at 40 wt.% PMMA.

Table 1: The values of energy gap (E_g), n, k, ϵ_r , and ϵ_i of (PAN/PMMA) blends with different blend ratios undoped and doped with 20 % of (Li_2CO_3 , $\text{Li}_2\text{SO}_4\cdot\text{H}_2\text{O}$, and LiCl)

Blend Ratios	Type of Salts	Energy Gap (E_g) (eV)	$\lambda=550$ nm			
			n	K	ϵ_r	ϵ_i
80%PAN+20%PMMA	Undoped	4	1.5	0.00026	2.42	0.00089
	Li_2CO_3 20 %	2.4	3.1	0.00132	7.68	0.00551
	$\text{Li}_2\text{SO}_4\cdot\text{H}_2\text{O}$ 20 %	3.2	5.0	0.00172	15.08	0.01096
	LiCl 20 %	3.1	5.8	0.002472	17.62	0.01368
75%PAN+25%PMMA	Undoped	4.1	1.53	0.000206	2.48	0.01305
	Li_2CO_3 20 %	2.4	3.15	0.00143	7.81	0.0550
	$\text{Li}_2\text{SO}_4\cdot\text{H}_2\text{O}$ 20 %	2.07	5.03	0.00213	14.96	0.0992
	LiCl 20 %	2.9	5.81	0.00423	17.56	0.1680
70%PAN+30%PMMA	Undoped	4.15	1.55	0.000141	2.54	0.340
	Li_2CO_3 20 %	2.3	3.17	0.00173	7.78	0.640
	$\text{Li}_2\text{SO}_4\cdot\text{H}_2\text{O}$ 20 %	3.1	5.05	0.00262	15.2	0.906
	LiCl 20 %	2.4	5.88	0.00323	17.56	1.352
65%PAN+35%PMMA	Undoped	4.16	1.7	0.00025	2.61	0.160
	Li_2CO_3 20 %	2.0	3.7	0.00156	8.5	0.337
	$\text{Li}_2\text{SO}_4\cdot\text{H}_2\text{O}$ 20 %	2.7	4.8	0.00258	14.6	0.549
	LiCl 20 %	3.0	5.4	0.00314	17.3	0.665
60 % PAN+40 % PMMA	Undoped	4.2	1.2	0.000191	1.43	0.00074
	Li_2CO_3 20 %	2.1	3.36	0.00196	11.8	0.0092
	$\text{Li}_2\text{SO}_4\cdot\text{H}_2\text{O}$ 20 %	2.9	5.3	0.00353	18.9	0.01800
	LiCl 20 %	3.3	6.3	0.00406	22.7	0.0260

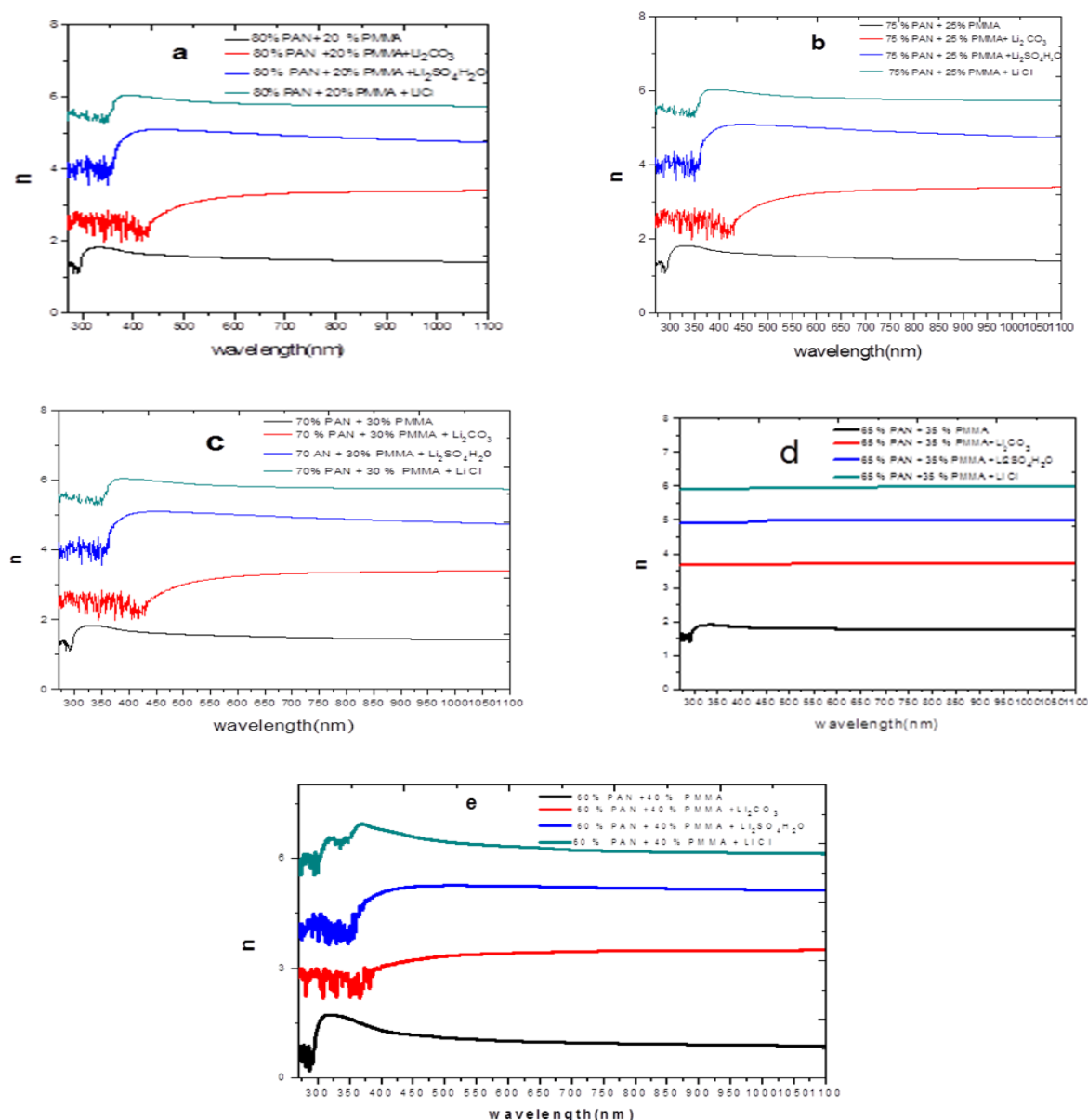


Figure 5: Refractive index versus wavelength for (PAN/ PMMA) blends with different blends ratios undoped and doped with 20% of Li_2CO_3 , $\text{Li}_2\text{SO}_4\text{H}_2\text{O}$, and LiCl

Extinction coefficient of (PAN/PMMA) blend with different ratios undoped and doped with different Lithium salts

Figure 6 illustrates the relationship between the extinction coefficient (k) and the wavelength (λ) of PMMA-PAN at different weight ratios and doped with Li_2CO_3 , $\text{Li}_2\text{SO}_4\text{H}_2\text{O}$ and LiCl lithium salts. The extinction coefficient of undoped (PAN/PMMA) blends reduced by increasing, followed by an increment by a further increase of PMMA, and finally reduced again for a high PMMA ratio. Indeed, the value of the extinction

coefficient (k) for the undoped polymer blend sample (80% PAN+20% PMMA) is (0.0026), decreases to 0.0020-0.00014 by increasing PMMA from 25% to 30%, and then increases from 0.00025-0.00196 at PMMA ratio increases to ratio 35%, 40%. It is noted that (k) decreases as the wavelength (λ) increases for undoped (PAN/PMMA) blend samples. It should be noted that (k) changes as the weight percentages of lithium salts are added to the host polymer. However, the increase of (k) values occurred in a non-systematic sequence. It can be seen that the extinction coefficient (k) values increase

irregularly for all samples doped with lithium salts but decrease irregularly with the blend's ratios of (PAN/PMMA) which are used. The behavior of the extinction coefficient (attenuation of incident photon intensity) is related to the scattering events that occur in blend samples.

Real and imaginary dielectric constant of (PAN/PMMA) blends with different blend ratios undoped and doped with different Lithium salts

The real ϵ_r and imaginary ϵ_i components of the dielectric constant as a function of wavelength are shown in Figure 7 and Figure 8 for (PAN/PMMA) at different blends ratios undoped and doped with various Lithium salts (Li_2CO_3 , $\text{Li}_2\text{SO}_4\cdot\text{H}_2\text{O}$, and LiCl). The variation of ϵ_r is primarily affected by the values of (n_2) as a result of the small (k_2) in the variation of ϵ_i is primarily influenced by the (k) values, which are related to the comparison with (n_2), whereas the variation of the absorption coefficient.

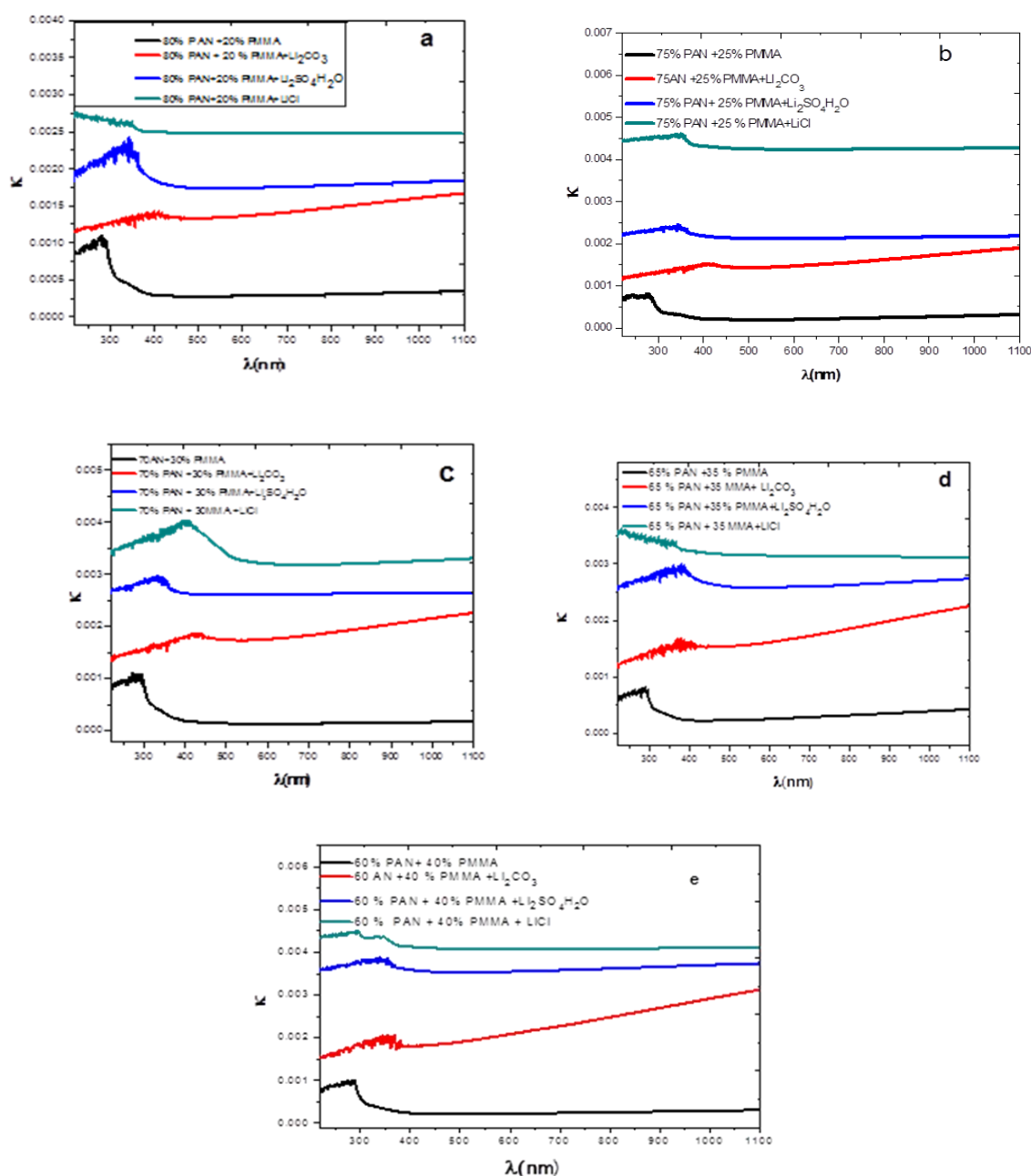


Figure 6: Extinction coefficient versus wavelength of (PAN/PMMA) blends with different blends ratios undoped and doped with 20 % of Li_2CO_3 , $\text{Li}_2\text{SO}_4\cdot\text{H}_2\text{O}$, and LiCl

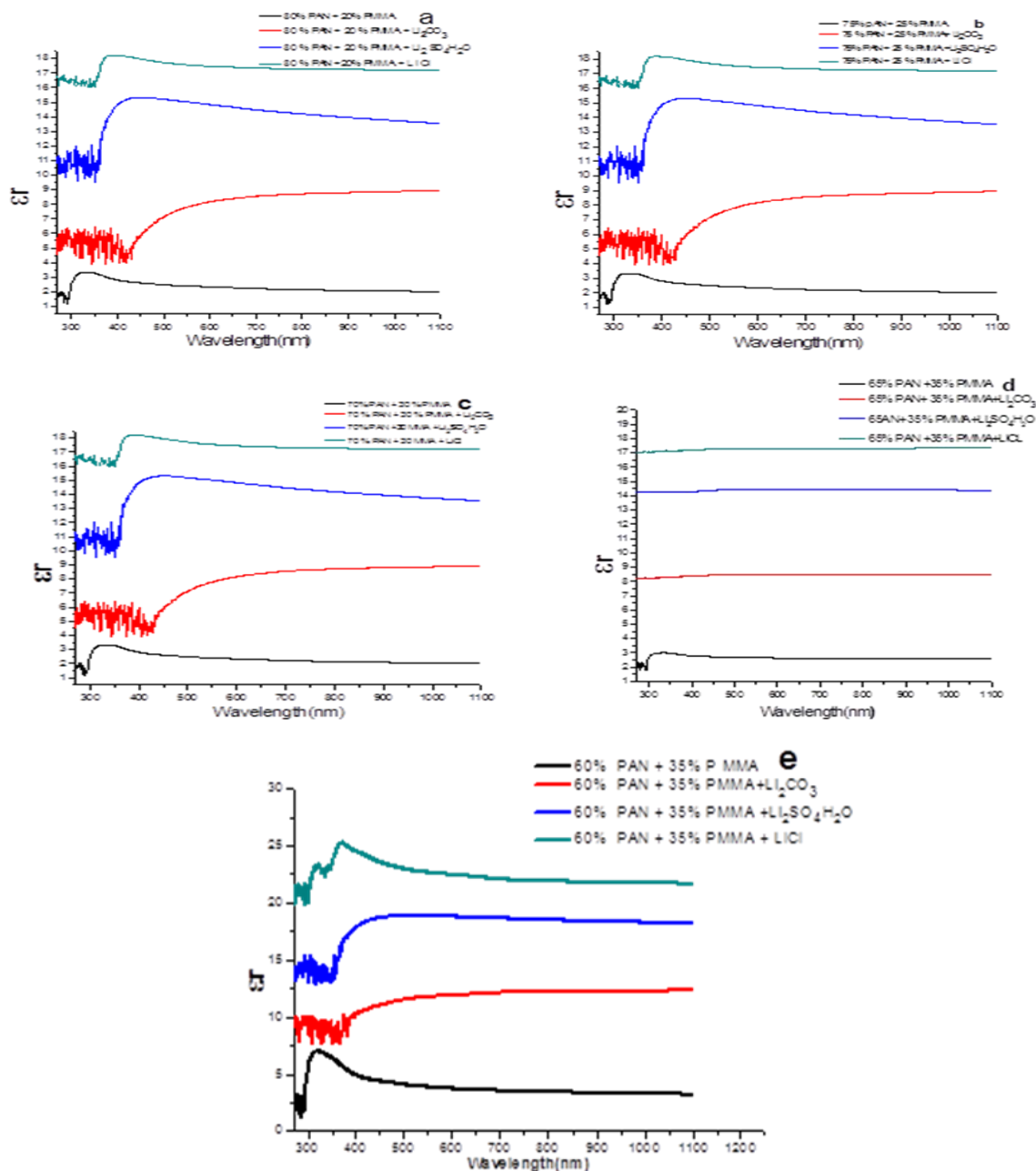


Figure 7: Variation of real dielectric constant versus wavelength of (PAN/PMMA) blends with different blends ratios undoped and doped with 20 % of Li_2CO_3 , $\text{Li}_2\text{SO}_4\cdot\text{H}_2\text{O}$ and LiCl

The values of ϵ_r increase with increasing in blend ratio; indeed, ϵ_r increases from 2.42 to 2.61 and as the ratio of PMMA increases from 20 to 35 % and then reduces to 1.43 with further increase in blend ratio. On the other hand, ϵ_r and ϵ_i values of doped samples are higher than those of undoped samples. It can be noticed from Figure 8 that the imaginary dielectric constant spectra become nearly-constant with wavelength change. It is

clear that the values (ϵ_r) and (ϵ_i) increase but in a non-systematic manner when lithium salts are added to the polymer blends, as shown in Table 1. The imaginary dielectric constant is defined as the loose part of the electromagnetic radiation after an incident on material; thus, when it becomes nearly constant, it becomes independent wavelength but depends on the type of filler only [27].

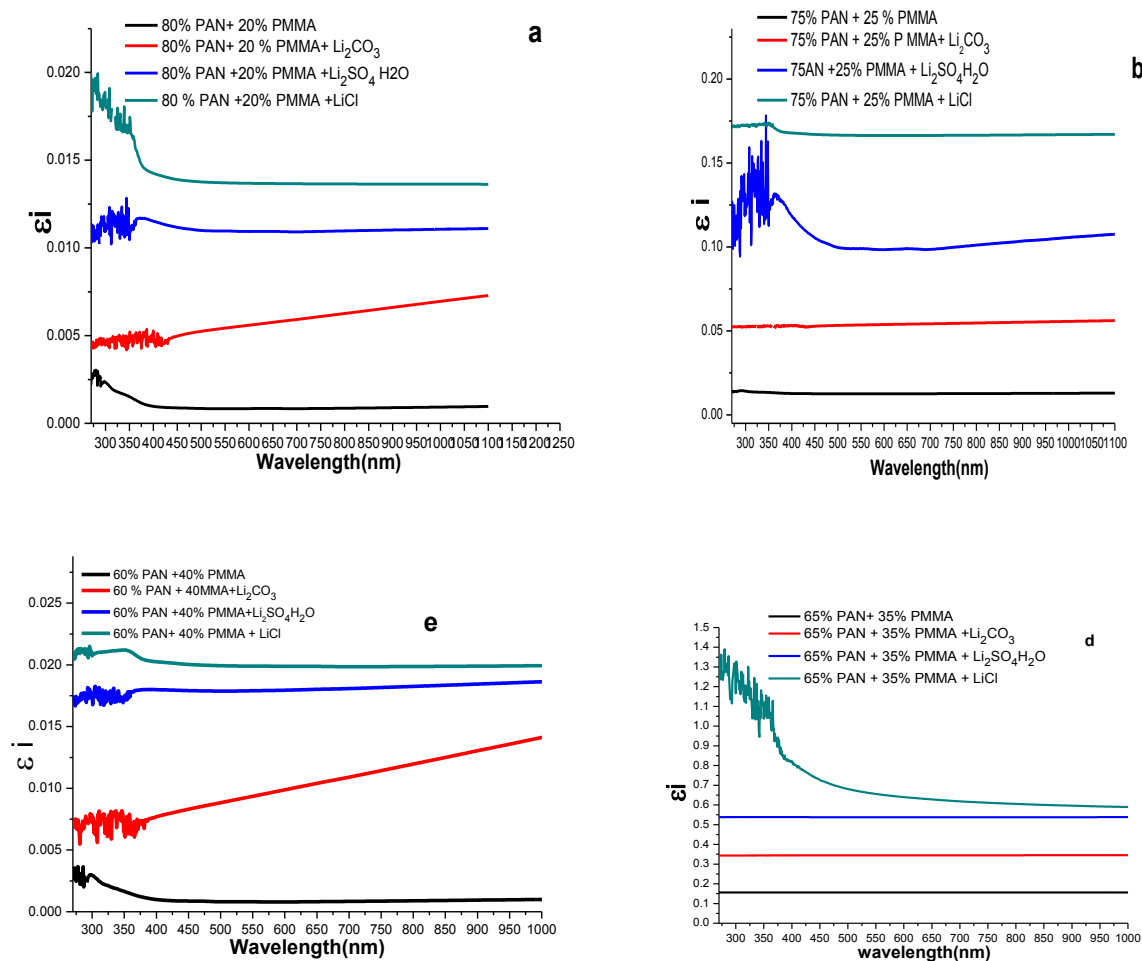


Figure 8: Variation of imaginary dielectric constant versus wavelength of (PAN/PMMA) blends with different blends ratios undoped and doped with 20 % of Li_2CO_3 , $\text{Li}_2\text{SO}_4\cdot\text{H}_2\text{O}$, and LiCl

Conclusion

The FT-IR spectrum confirmed the introduction of lithium salts to the host polymer blends. The addition of PMMA made the blend samples more transparent to the incident radiation throughout, shifting the energy gap values toward the high-energy side. In contrast, the addition of lithium salts made the blend samples opaque to the incident radiation throughout, shifting the energy gap toward the low-energy side. The optical constant was significantly affected by the increase in blend ratio and the doping with various lithium Salts.

Acknowledgements

We would like to thank Dr. Bushra Abbas Hasan and the College of Science and Department of Physics at Baghdad University and Dr. Eman

Hashimkhader from University of Technology for their support during this work.

Funding

This research did not receive any specific grant from funding agencies in the public, commercial, or not-for-profit sectors.

Authors' contributions

All authors contributed to data analysis, drafting, and revising of the paper and agreed to be responsible for all the aspects of this work.

Conflict of Interest

There are no conflicts of interest in this study.

ORCID:

Raad H. Khudher

<https://orcid.org/0000-0001-9125-6789>

Ahmad A. Hasan

<http://orcid.org/0000-0001-5384-9743>

References

- [1]. Syed T., Thelakkadan A.S., Al-Hussain S., Date-Palm Fiber as a Reinforcement Filler in Polymer Composites, *Advances in Sciences and Engineering*, 2020, **12**:78 [[Crossref](#)], [[Google Scholar](#)], [[Publisher](#)]
- [2]. Rahman M.H., Werth H., Goldman A., Hida Y., Diesner C., Lane L., Menezes P.L., Recent Progress on Electroactive Polymers: Synthesis, Properties and Applications, *Ceramics*, 2021, **4**:516 [[Crossref](#)], [[Google Scholar](#)], [[Publisher](#)]
- [3]. Abbrent S., Greenbaum S., Peled E., Golodnitsky D., Polymer electrolytes, *Handbook of Solid State Batteries*, 2016, **1**:523 [[Crossref](#)], [[Google Scholar](#)], [[Publisher](#)]
- [4]. Hallinan Jr D.T., Balsara N.P., Polymer electrolytes, *Annual Review of Materials Research*, 2013, **43**:503 [[Crossref](#)], [[Google Scholar](#)], [[Publisher](#)]
- [5]. Kim C.S., Oh S.M., Importance of donor number in determining solvating ability of polymers and transport properties in gel-type polymer electrolytes, *Electrochimica Acta*, 2000, **45**:2101 [[Crossref](#)], [[Google Scholar](#)], [[Publisher](#)]
- [6]. Karvounis A., Grange R., Electro-mechanical to optical conversion by plasmonic-ferroelectric nanostructures, *Nanophotonics*, 2022 [[Crossref](#)], [[Google Scholar](#)], [[Publisher](#)]
- [7]. Mohamadinooripoor R., Kashanian S., Moradipour P., Sajadimajd S., Arkan E., Tajehmiri A., Rashidi K., Novel elastomeric fibrous composites of poly-ε-caprolactone/propolis and their evaluation for biomedical applications, *Journal of Polymer Research*, 2022 **29**:1 [[Crossref](#)], [[Google Scholar](#)], [[Publisher](#)]
- [8]. Das D., Samanta S., Complex Dielectric Characteristics, ac-Conductivity, and Impedance Spectroscopy of B-Doped NC-SiO X: H Thin Films, *ACS Applied Electronic Materials*, 2021 **3**:1634 [[Crossref](#)], [[Google Scholar](#)], [[Publisher](#)]
- [9]. Yu X., Manthiram A., A review of composite polymer-ceramic electrolytes for lithium batteries, *Energy Storage Materials*, 2021, **34**:282 [[Crossref](#)], [[Google Scholar](#)], [[Publisher](#)]
- [10]. Abeykoon N.C., Bonso J.S., Ferraris J.P., Supercapacitor performance of carbon nanofiber electrodes derived from immiscible PAN/PMMA polymer blends, *Rsc Advances*, 2015, **5**:19865 [[Crossref](#)], [[Google Scholar](#)], [[Publisher](#)]
- [11]. Rajendran S., Shanker B. R., Sivakumar P., Investigations on PVC/PAN composite polymer electrolytes, *Journal of Membrane Science*, 2008, **315**:67 [[Crossref](#)], [[Google Scholar](#)], [[Publisher](#)]
- [12]. Fryczkowska B., Piprek Z., Sieradzka M., Fryczkowski R., Janicki J., Preparation and properties of composite PAN/PANI membranes, *International Journal of Polymer Science*, 2017, **2017**:3257043 [[Crossref](#)], [[Google Scholar](#)], [[Publisher](#)]
- [13]. Athal M.A., Hanoosh W.S., Abdullah A.Q., Analysis of band gap energy and refractive index of electrospinning polyacrylonitrile (PAN) nanofibers, *Basrah Journal of Science*, 2020, **38**:111 [[Google Scholar](#)], [[Publisher](#)]
- [14]. Raghavendra S.C., Khasim S., Revanasiddappa M., Ambika M.V., Kulkarni A.B., Synthesis, characterization and low-frequency ac conduction of polyaniline/fly ash composites, *Bulletin of Materials Science*, 2003, **26**:733 [[Crossref](#)], [[Google Scholar](#)], [[Publisher](#)]
- [15]. Patterson J., Bailey B., Solid-state physics: introduction to the theory, Springer Science & Business Media, 2007 [[Google Scholar](#)], [[Publisher](#)]
- [16]. Rouaramadan E., Hasan A.A., Study of the optical constants of the PVC/PMMA blends, *International Journal of Application or Innovation in Engineering & Management*, 2013, **2**:240 [[Google Scholar](#)], [[Publisher](#)]
- [17]. Hazim A., Hashim A., Abduljalil H., Fabrication of novel (PMMA-Al₂O₃/Ag) nanocomposites and its structural and optical properties for lightweight and low-cost electronics applications, *Egyptian Journal of Chemistry*, 2021, **64**:359 [[Crossref](#)], [[Google Scholar](#)], [[Publisher](#)]
- [18]. Alwan T.J., Gamma irradiation effect on the optical properties and refractive index dispersion of dye doped polystyrene films, *Turkish Journal of*

- Physics, 2012, **36**:377 [[Crossref](#)], [[Google Scholar](#)], [[Publisher](#)]
- [19].AlFannakh H., Impedance Spectroscopy, AC Conductivity, and Conduction Mechanism of Iron Chloride/Polyvinyl Alcohol/Polyvinylpyrrolidone Polymer Blend, *Advances in Materials Science and Engineering*, 2022, **2022**:7534935 [[Crossref](#)], [[Google Scholar](#)], [[Publisher](#)]
- [20].Lin-Vien D., Colthup N.B., Fateley W.G., Grasselli J.G., *The handbook of infrared and Raman characteristic frequencies of organic molecules*, Academic Press, New York, 1991 [[Crossref](#)], [[Google Scholar](#)], [[Publisher](#)]
- [21].Siddaiah T., Ojha P., Gopal N.O., Ramu C., Nagabhushana H., Thermal, structural, optical and electrical properties of PVA/MAA: EA polymer blend filled with different concentrations of Lithium Perchlorate, *Journal of Science, Advanced Materials and Devices*, 2018, **3**:456 [[Crossref](#)], [[Google Scholar](#)], [[Publisher](#)]
- [22].Mettu M.R., Mallikarjun A., Reddy M.V., Reddy M.J., Kumar J.S., Investigation of Structural and Optical Properties of PMMA/PVdF-HFP Polymer Blend System, In *Proceedings of Fourth International Conference on Inventive Material Science Applications*, Springer, Singapore, 2022, **1**:295 [[Crossref](#)], [[Google Scholar](#)], [[Publisher](#)]
- [23].Wang W., Zheng Y., Sun Y., Jin X., Niu J., Cheng M., Wang H., Shao H., Lin T., High-temperature piezoelectric conversion using thermally stabilized electrospun polyacrylonitrile membranes, *Journal of Materials Chemistry A*, 2021, **9**:20395 [[Crossref](#)], [[Google Scholar](#)], [[Publisher](#)]
- [24].Hashim A., Hadi Q., Structural, electrical and optical properties of (biopolymer blend/titanium carbide) nanocomposites for low-cost humidity sensors, *Journal of Materials Science: Materials in Electronics*, 2018, **29**:11598 [[Crossref](#)], [[Google Scholar](#)], [[Publisher](#)]
- [25].Hashim A., Abbas B., Recent review on polymethyl methacrylate (PMMA)-polystyrene (PS) blend doped with nanoparticles for modern applications, *Research Journal of Agriculture and Biological Sciences*, 2019, **14**:6 [[Crossref](#)], [[Google Scholar](#)], [[Publisher](#)]
- [26].Abbas Y.M., Hasan A.A., Optical Properties Study of Polypyrrole doped with TiO₂, WO₃, Fe₂O₃ and SnO₂ Nanoparticles, In *IOP Conference Series: Materials Science and Engineering*, 2020, **928**:72017 [[Crossref](#)], [[Google Scholar](#)], [[Publisher](#)]
- [27].Manjuladevi R., Thamilselvan M., Selvasekarapandian S., Mangalam R., Premalatha M., Monisha S., Mg-ion conducting blend polymer electrolyte based on poly (vinyl alcohol)-poly (acrylonitrile) with magnesium perchlorate, *Solid State Ionics*, 2017, **308**:90 [[Crossref](#)], [[Google Scholar](#)], [[Publisher](#)]

HOW TO CITE THIS ARTICLE

Raad H. Khudher, Ahmad A. Hasan. Effect of Lithium Salts on the Optical Properties of Poly Acrylonitrile/Poly Methyl Methacrylate Blends. *Chem. Methodol.*, 2022, 6(11) 872-885
 DOI: <https://doi.org/10.22034/CHEMM.2022.354600.1587>
 URL: http://www.chemmethod.com/article_155074.html